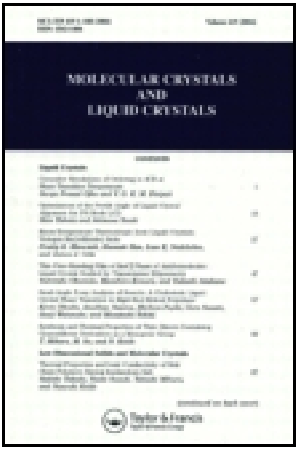

Molecular Crystals and Liquid Crystals
Publication details, including instructions for authors and subscription information:
http://www.tandfonline.com/loi/gmcl20

Chip-On-Glass Bonding Using Sn Bump and Non-Conductive Adhesive for LCD Application

Bae-Yong Kim [a], Zhigang Chen [a] & Young-Ho Kim [a]
[a] Division of Materials Science & Engineering, Hanyang University, Seoul, Korea

Version of record first published: 21 Dec 2006

Mol. Cryst. Liq. Cryst., Vol. 458, pp. 199–206, 2006

ISSN: 1542-1406 print/1563-5287 online
DOI: 10.1080/15421400600932363

Taylor & Francis
Taylor & Francis Group

Chip-On-Glass Bonding Using Sn Bump and Non-Conductive Adhesive for LCD Application

Bae-Yong Kim
Zhigang Chen
Young-Ho Kim
Division of Materials Science & Engineering, Hanyang University, Seoul, Korea

We developed a new chip-on-glass (COG) bonding method using non-conductive adhesive (NCA) and Sn bumps. The bonding was performed with various electrode pads on the glass substrate at 150°C for 150 s under 100 MPa. The initial average contact resistance was 5.7 mΩ for Au pad, 19.6 mΩ for indium-tin oxide (ITO)/Au pad, 11.2 mΩ for Al pad respectively. Thermal cycling test was performed in the temperature range between 0°C and 100°C. The contact resistance of the Sn bump-Au pad joints did not change even after 1000 cycles. In contrast, the joints formed on other type of pads failed electrically between 300 and 500 cycles.

Keywords: chip-on-glass (COG); non-conductive adhesive (NCA); Sn bump; thermal cycling

INTRODUCTION

Packaging technology for flat panel display (FPD) drivers has evolved from tape automated bonding (TAB) to chip-on-glass (COG) for reasons of cost, size, and performance [1]. In the case of TAB technology, one of the limiting factors is the dimensional instability of the polyimide carrier of the TAB tape in fine pitch interconnection [2]. However, in the case of COG technology, the integrated circuit (IC) chips are bonded directly to the glass substrate of the liquid crystal display (LCD) panel. As a result, COG can satisfy many requirements for an ideal assembly process. One advantage of COG is the reduction in

This work was supported by the Korea Research Foundation Grant (KRF-2004-005-D00164).
Address correspondence to Young-Ho Kim, Division of Materials Science & Engineering, Hanyang University, Seoul 133-791, Korea. E-mail: kimyh@hanyang.ac.kr

packaging cost for the display module compared to TAB [3]. Another advantage is that finer pitches are able to be bonded [4]. Also, COG technology allows the driver to be bonded directly to the indium-tin oxide (ITO) traces on the glass without increasing the size of the panel. Thus the use of COG technology reduces the size of the packaged FPD module [3]. Generally, COG bonding technique utilizes Au bump and anisotropic conductive film (ACF) due to fine pitch capability and good electrical performance [5]. Also, ACF bonding has several advantages such as low temperature, simple process, lead-free and fluxless bonding process. However, in the case of ultrafine pitch packaging for high-definition LCDs, the failure caused by the electrical short and opening may be issued in the COG technique using ACF. Also, the contact resistance will increase due to the reduction of contact area. Recently, COG technology using non-conductive adhesive (NCA) has been introduced as one of the most suitable interconnection method for fine pitch packaging, since the bumps and electrode pads can be contacted directly. Au or Au/Ni bumps are generally used as conductive metal bumps [6,7]. However, in this study, we used Sn as bump material, since Sn bump has higher plastic deformation capability than Au bump, which was targeted to compensate for the bump height ununiformity, a concern when performing NCA flip chip bonding. Also, low manufacturing cost is another consideration in using Sn bump. The reliability of NCA applied COG joints was evaluated from thermal cycling test.

EXPERIMENTAL PROCEDURE

Au (50 nm)/Cu (1 μm)/Ti (50 nm) thin films were deposited on SiO_2/Si wafer for conductive lines using DC magnetron sputtering. The conductive lines were fabricated through the photolithographic process and wet chemical etching. The Sn bumps were formed on the conductive lines using evaporation method, followed by lift-off process. The Sn bump size was 100 μm square and 10 μm in thickness. Three types of electrode pads, Au (50 nm)/Cu (1 μm)/Ti (50 nm), indium-tin oxide (ITO) (100 nm)/ Au (50 nm)/Cu (1 μm)/Ti (50 nm), and Al (1 μm), were formed on glass substrates using DC magnetron sputtering. Non-conductive adhesive (NCA) was dispensed on the surface of Sn bumps, and then the bonding process was performed at 150°C for 150 s under 100 MPa, using thermocompression bonder. Figure 1 summarizes the basic process flow. The contact resistance was measured using four-point probe method at room temperature. For the reliability evaluation, thermal cycling tests (0°C–100°C, 30 min/cycle) up to 1000 cycles were carried out. During the thermal cycling test, the variation of the contact resistance of the joints was measured every 100 cycles.

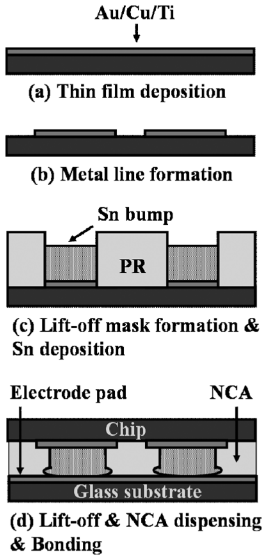

FIGURE 1 Schematic diagram showing the boning process.

The microstructure of COG joints before and after thermal cycling was characterized, and the failure mechanism of joints after thermal cycling was analyzed using scanning electron microscopy (SEM) with the energy dispersive spectrometry (EDS).

RESULTS

A. Contact Resistance of COG Joints with Different Pads

The initial average contact resistance was 5.7 mΩ for Au pad, 19.6 mΩ for ITO/Au pad, 11.2 mΩ for Al pad, respectively. The contact resistance values of all joints were much lower than that of conventional anisotropic conductive film (ACF) regardless of the type of electrode pads [8,9]. The average contact resistance of Sn-ITO joints is higher than those of Sn-Au joints and Sn-Al joints due to the high sheet resistance of ITO. In the case of Sn-Au joints, the average contact resistance remained almost unchanged before and after thermal cycling. Even after 1000 cycles, the value was still around 5.6 mΩ. And, no evidence of failure was observed. However, the trend of the contact resistance change in the other joints during thermal cycling was different in comparison with Sn-Au joints. The average contact resistance of Sn-ITO pad joints did not increase up to 300 cycles, but the contact resistance increased sharply after 400 cycles, with the

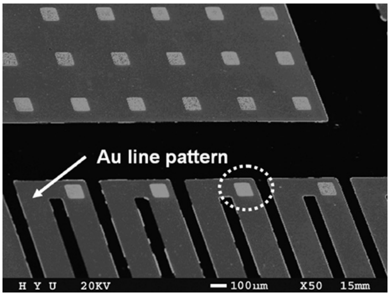

FIGURE 2 A SEM image showing the metal lines and Sn bumps.

value of 1 Ω to several kΩ. Also, the similar phenomenon was found in the Sn-Al pad joints. The contact resistance remained nearly unchanged up to 300 cycles and then increased from 11.2 mΩ to 583 mΩ after 400 cycles. In addition, after 500 cycles, this value changed to about 1 Ω to 1 kΩ. Conclusively, all joints formed between Sn bumps and ITO or Al pads failed electrically after 500 cycles.

B. Microstructure of COG Joints Before and After Thermal Cycling

Figure 2 is a SEM image showing the Au/Cu/Ti conductive lines and Sn bumps formed successfully on conductive lines. Figure 3 is a SEM image showing a typical COG joint formed using Sn bump and NCA. Sn bumps on the Si was successfully contacted with the conductive pads on the glass substrate. Figure 4 is a detailed image of the COG joint formed between Sn bump and Au pad before thermal cycling. The interfacial intermetallic compounds were found at the interfaces. During bonding, heat and pressure was applied and active solid state diffusion occurred between Sn bump and Au pad as well as between Sn bump and under bump metallurgy (UBM). Therefore, as shown in Figure 4, intermetallic compounds (IMCs) formed at Sn bump/Au

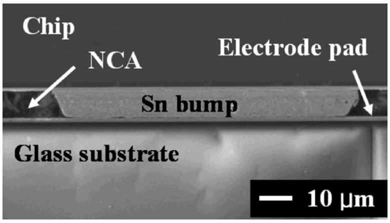

FIGURE 3 A typical SEM image showing the COG joint with NCA.

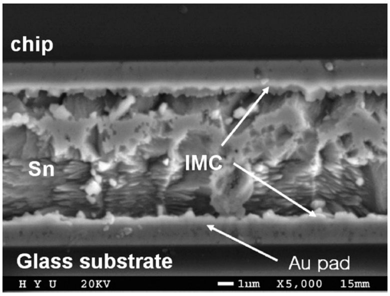

FIGURE 4 A cross-sectional SEM image showing Sn bump-Au pad joint before thermal cycling.

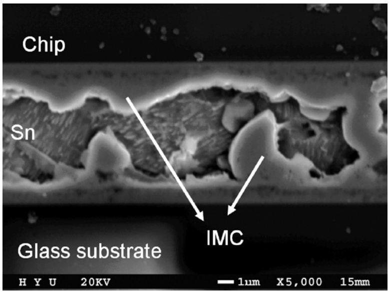

FIGURE 5 A cross-sectional SEM image showing Sn bump-Au pad joint after thermal cycling.

pad interface and Sn bump/UBM interface [10]. These IMCs were identified to be (Au, $Cu)_6Sn_5$. On the other hand, IMCs did not form at the Sn bump/ITO pad and Sn bump/Al pad interfaces since no reaction was expected to take place between Sn and ITO or Sn and Al.

Figure 5 is a SEM image showing the cross-section of Sn bump to Au pad joint after 1000 cycles. During the thermal cycling, the IMC at Sn bump/Au pad interface thickened and this phase remained as (Au, $Cu)_6Sn_5$. In the Sn-ITO and the Sn-Al joints, the delamination between bumps and pads during thermal cycling was observed, as shown in Figure 6.

DISCUSSION

Failure Mechanism

The intermetallic compounds formed at the solder/substrate interfaces are usually regarded as weak site, where the microcracks

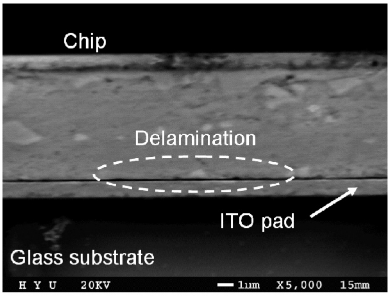

(a)

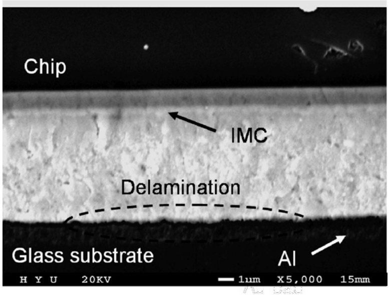

(b)

FIGURE 6 Cross-sectional SEM images showing (a) Sn bump-ITO pad joint and (b) Sn bump-Al pad after thermal cycling.

originate and propagate and finally result in the failure of joints especially in the thermal cycling due to the thermal expansion mismatch between the chip and substrate. In order to improve the reliability of solder joints, underfill materials are preferred to be applied between the chip and substrate to distribute the thermal stress across the entire chip rather than the joints alone. Thus, the thermal expansion mismatch will be remarkably reduced. NCA bonding can be regarded as a pre-applied underfill process as well. Another benefit of using NCA lies on that it can provide a compressive force created by the shrinkage of NCA after being cured.

In the cases of Sn-Al joints and Sn-ITO joint, the conductivity of the interconnect relied highly on the mechanical contact between bumps and pads. This mechanical contact was "zero strength" contact and was sustained by the compressive force supplied by the NCA. Therefore, the properties of NCA would directly influence the quality of Sn-Al and Sn-ITO joints. However, the degradation of NCA during temperature variation will lead to the stress relaxation of this compressive force [3]. The stress relaxation in the NCA will finally result in a time dependant drop in the compressive force and hence in a corresponding increase of the contact resistance [11]. Additionally, recent study showed that cyclic relaxation has dependency on hold time, no-load time and ramp rate of the thermal cycling [12]. As the NCA relaxed, the delamination would occur, resulting in the final electrical failure of the joints.

In contrast, the joints made by Sn bumps and Au pads exhibit excellent reliability. The Sn-Au pad joints can endure stress caused by thermal mismatch partly due to the stress distribution effect of NCA. On the other hand, it is not mechanical contact but metallurgical bonding. The interfacial intermetallic compounds provided higher strength compared with the mechanical contact. The thermal cycling results of Sn-Au joints indicated that additional metallurgical reaction at the interfaces would enhance the interconnection during the thermal cycling, compensating for the degradation of compressive force due to the relaxation of NCA.

CONCLUSIONS

The reliability of Sn-Au, Sn-ITO, and Sn-Al pad joints was investigated. The microstructure of COG joints was characterized before and after thermal cycling. The main results are summarized as follows.

1. The average contact resistance of Sn-Au pad, Sn-ITO, Sn-Al pad joints was 5.7 mΩ, 19.6 mΩ, and 11.2 mΩ, respectively, which was much lower than that of the conventional ACF bonding.
2. Sn-ITO/Au pad and Sn-Al pad joints failed electrically between 300 and 500 cycles, but Sn-Au pad joints passed the thermal cycling test by 1000 cycles.
3. After bonding, $(Au, Cu)_6Sn_5$ IMCs was observed as a result of solid-state diffusion between bumps and Au pads. It also achieved remarkable growth during thermal cycling.

REFERENCES

[1] Hwang, J. C. (1995). Advanced low-cost bare-die packaging technology for liquid crystal displays. *IEEE Trans. Comp. Packag. Manufact. Technol. Part. A*, *18*(3), 458–461.

[2] Kang, U. B. & Kim, Y.-H. (2004). A new COG technique using low temperature solder bumps for LCD driver IC packaging applications. *IEEE. T. Compon. Pack. T*, *27*(2), 253–258.

[3] Kristiansen, H. & Liu, J. (1998). Overview of conductive adhesive interconnection technologies for LCDs. *IEEE Trans. Comp. Packag. Manufact. Technol. A*, *21*(2), 208–214.

[4] Bessho, Y., Horio, Y., Tsuda, T., Ishida, T., & Sakurai, W. (1990). Chip-on-glass mounting technology of LSI's for LCD module, In: *Proc. Int. Microelectron. Conf.*, 183–189.

[5] Chan, Y. C. & Luk, D. Y. (2002). Effects of bonding parameters on the reliability performance of anisotropic conductive adhesive interconnects for flip-chip-on-flex packages assembly II. Different bonding pressure. *Microelectron. Reliab.*, *42*(18), 1195–1204.

[6] Hsieh, Y.-T. (2002). Reliability and failure mode of chip-on-film with non-conductive adhesive, *Proceedings of the 4th International Symposium on Electronic Materials and Packaging*, 157–160.

[7] Kristiansen, H., Gulliksen, M., Haugerud, H., & Friberg, R. (1998). Characterisation of electrical contacts made by non-conductive adhesive, Adhesive Joining and Coating Technology in Electronics Manufacturing, Proceedings of 3rd International Conference, 345–350.

[8] Wojciechowski, D., Vanfleteren, J., Reese, E., & Hagedorn, H.-W. (2000). Electroconductive adhesives for high density package and flip-chip interconnections. *Microelectron. Reliab.*, *40*, 1215–1226.

[9] Yin, C. Y., Alam, M. O., Chan, Y. C., Bailey, C., & Lu, H. (2003). The effect of reflow process on the contact resistance and reliability of anisotropic conductive film interconnection for flip chip on flex applications. *Microelectron. Reliab.*, *43*, 625–633.

[10] Huh, J.-Y., Han, S.-U., & Park, C.-Y. (2004). Effect of Bismuth on the growth kinetics of intermetallic compounds in Sn-3.5Ag solder joints: A growth kinetic model. *Met. Mater-Int.*, *10*(2), 123–132.

[11] Caers, J. F. J. M., Zhao, X. J., Hansen, G. Sy., Wong, E. H., & Mhaisalkar, S. G. (2004). Towards a predictive behavior of non-conductive adhesive interconnects in moisture environment. *Electron. Compon. Techn. Confer.*, 106–112.

[12] Gunawana, M., Davilaa, L. T., Wongb, E. H., Mhaisalkara, S. G., Tsaic, T. K., & Osiyemi, S. (2004). Static and cyclic relaxation studies in nonconductive adhesives. *Thin Solid Films*, *462/463*, 419–426.